Magnetic Stars, 2011, pp. 69 – 80

Modelling the Atmospheres of Peculiar Magnetic Stars

Ryabchikova T.[1], **LeBlanc F.**[2], **Shulyak D.**[3]

[1] Institute of Astronomy RAS, Moscow, Russia
[2] Département de Physique et d'Astronomie, Université de Moncton, Moncton, Canada
[3] Institute of Astrophysics, Georg–August–University, Göttingen, Germany

Abstract. A review of the status in modelling the atmospheres of magnetic peculiar stars is given. Two kinds of models are considered: modelling with individual chemical anomalies and an empirically derived stratification for the most important elements based on the LLmodels code, and self–consistent diffusion models based on the Phoenix code, where a theoretical stratification of 39 elements is calculated simultaneously with model atmosphere calculations. We show that the LLmodels which takes into account individual abundance anomalies provides an adequate description of the most anomalous observed energy distributions in Ap stars. Fitting the observed distribution, we get an accurate independent estimate of the global stellar parameters such as the radius, effective temperature and luminosity. For two Ap stars α Cir and γ Equ the stellar radii derived from the spectroscopic analysis agree very well with the direct interferometric measurements of radii. It gives us a powerful method for the radius determinations in Ap stars. Self–consistent diffusion models based on theoretical diffusion calculations in Ap atmospheres predicted the overall observed trends in Fe–peak element abundances with the effective temperature. The observed individual abundance anomalies in the hot Ap star HD 170973 agree well with the diffusion model predictions.

Key words: stars – magnetic chemically peculiar stars – spectroscopy – model atmospheres – diffusion – element stratification

1 Introduction

Magnetic chemically peculiar (Ap) stars have anomalously strong spectral lines of many chemical species in their spectra. Lines of the Fe–peak elements are dominated in the spectra of hotter Ap stars ($T_{\rm eff} = 9000 - 12000$ K) while for the cooler Ap stars numerous lines of the rare-earth elements start to play a more significant role in the line opacity. A constant increase of accuracy in different techniques used to observe Ap stars such as space photometry, spectroscopic monitoring for pulsations and magnetic field measurements requires an adequate improvement in the analysis of observational data, which is impossible without a corresponding improvement in the modelling of stellar atmospheres. One of the main problems for stellar atmosphere modelling is a huge amount of spectral lines which have to be taken into account — up to a hundred millions in the Ap atmospheres. Because of the specific abundance anomalies in Ap stars, where some elements may have abundances, enhanced by orders of magnitude compared to the solar ones, while the others may be underabundant, model atmosphere calculations based on the solar-scaled abundances and Opacity Distribution Function (ODF) method (Kurucz ATLAS9 code, for example) cannot provide an adequate description of the observed spectrum and energy distribution. An additional difficulty in Ap stars is created by the observed steep abundance gradients in their atmospheres (Wade et al., 2001; Ryabchikova et al., 2002). These abundance gradients are built by the diffusion processes (Michaud, 1970).

The first approach presented here uses abundances and element stratifications derived from the spectral observations, which are then included in the line opacity calculations realised by the LLmodels code (Shulyak et al., 2004). The second approach is purely theoretical and takes into account the element stratification caused by the diffusion process. These models are based on the Phoenix (Hauschildt et al., 1999) model atmospheres, where the diffusion of 39 chemical elements from He to La was calculated simultaneously and self–consistently with the structure of the model atmosphere (Hui–Bon–Hoa et al., 2000; LeBlanc, 2003; LeBlanc & Monin, 2005; LeBlanc et al., 2009). These models were successful in explaining several observational anomalies of blue horizontal branch stars (Hui–Bon–Hoa et al., 2000, LeBlanc et al. 2010). Alecian & Stift (2007, 2010) and LeBlanc et al. (2009) analysed the effect of the horizontal magnetic field on the element distribution due to the fact that ion diffusion velocities are modified when they cross the magnetic lines. Alecian & Stift (2007, 2010) also included the Zeeman effect in their calculations, but , however, did not calculate the atmospheric structure self–consistently with the predicted elemental stratification.

In this paper we review the recent results of modelling the atmospheres of Ap stars.

2 Empirical LLmodels

A detailed description of modelling of the empirical LLmodels is given by Kochukhov et al. (2009). The following steps are done for each star:

Step 1: a calculation of a model atmosphere grid using mean abundances derived in previous studies;

Step 2: a determination of $T_{\rm eff}$ and $\log g$ with the help of spectrophotometry, Balmer line profiles and broad–band colours;

Step 3: a determination of average abundances and chemical stratification using high–resolution spectra;

Step 4: a calculation of a new model atmosphere grid, taking into account individual abundances and stratification, found in the previous step;

Step 5: repeating the entire process starting from Step 2 until convergence is achieved.

Model calculations are carried out with the LLmodels code (Shulyak et al., 2004), while the stratification analysis is performed with the DDAFit code written by O. Kochukhov (see Ryabchikova et al., 2005 for details). Calculations of the theoretical element distributions by Babel (1992) provided the step–like shape of the abundance profiles, which was employed in the empirical stratification studies with the DDAFit code. The model atmosphere grids are calculated for the $T_{\rm eff}$ range of $7000-8000$ K with a 200 K step and for $\log g = 3.8-4.2$ with a 0.1 dex step. We adopted the convergence criterion of the absence of significant variations of the mean abundances, stratification profiles of studied chemical elements and model atmosphere parameters. The modelling process is iterative, and the convergence is usually achieved within 3 iterations. The final self–consistent, chemically–stratified model atmosphere is expected to reproduce simultaneously the observed photometry, energy distribution, hydrogen line profiles and metallic line spectra.

Below we discuss the results of the atmospheric modelling of four cool Ap stars.

2.1 α Cir

α Cir was the first star for which we performed model atmosphere calculations with the LLmodels code taking into account individual abundances and element stratification for Si, Ca, Cr and Fe.

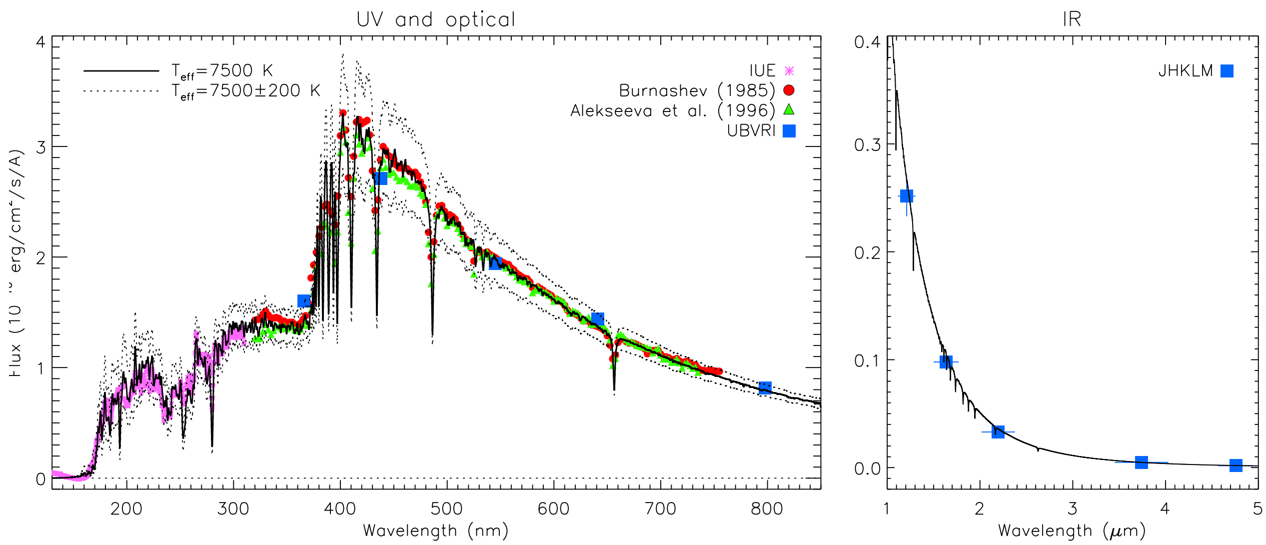

Figure 1: Comparison between the observed (*symbols*) and theoretical (*lines*) spectral energy distributions of α Cir. Photometric and spectrophotometric observations cover the wavelength range from the ultraviolet and optical (*left panel*) to the infrared (*right panel*). The solid line shows the theoretical energy distribution computed for the final self–consistent model atmosphere of α Cir with parameters $T_{\rm eff} = 7500$ K and $\log g = 4.1$. The dotted lines illustrate the effect of changing $T_{\rm eff}$ by ± 200 K. The LLMODELS flux spectra are convolved with a FWHM = 10 Å Gaussian profile.

After 3 iterations, the model with $T_{\rm eff} = 7500 \pm 130$ K and $\log g = 4.1 \pm 0.15$ was chosen as the best one representing the observed energy distribution in this star (Kochukhov et al., 2009). Fig. 1 (taken from Kochukhov et al., 2009) demonstrates the quality of our model. A fit of the theoretical energy distribution to the observed spectrophotometry taken from the IUE archive and databases of Burnashev (1985) and Alekseeva et al. (1996) give us a radius of the star if we apply the known Hipparcos parallax $\pi = 60.36 \pm 0.14$ mas from van Leeuwen (2007). With this procedure we get $R = 1.947 \pm 0.064 R_\odot$ which is in excellent agreement with the value $R = 1.967 \pm 0.066 R_\odot$ derived from the direct interferometric measurements (Bruntt et al., 2008). Note that the newly derived effective temperature of α Cir is 400 K is lower than the previous determination by Kupka et al. (1996).

The chemical stratification has a noticeable impact on the model structure and modifies the formation of the hydrogen Balmer lines (see Fig. 2 taken from Kochukhov et al., 2009). At the same time, energy distribution appears to be less sensitive to the presence of large abundance gradients.

2.2 HD 24712

A rapidly oscillating (roAp) star HD 24712 is the second star for which a detailed modelling of the atmosphere was performed. In this star, stratification of 8 elements was derived: Si, Ca, Cr, Fe, Sr, Pr, Nd. For the two rare–earth elements (REE) Pr and Nd a stratification analysis was made in the NLTE approximation by the trial–and–error method, while in the model atmosphere calculations the NLTE effects were roughly simulated by the simple scaling of $\log(gf)$ values of REE lines depending on the ionization stage of the respective element. We refer the reader to the paper by Shulyak et al. (2009) for more details. The observed anomalies in the intensity of REE lines in the first and second ionization stages can only be explained by the enhanced REE abundance in the upper atmospheric layers. Fig. 3 shows the final element distribution in the HD 24712 atmosphere and its impact on the temperature structure. Fig. 4 shows a fit of the theoretical flux to the observed one. Combined with the Hipparcos parallax $\pi = 20.32 \pm 0.39$ mas (van Leeuwen, 2007) it leads to the radius estimate

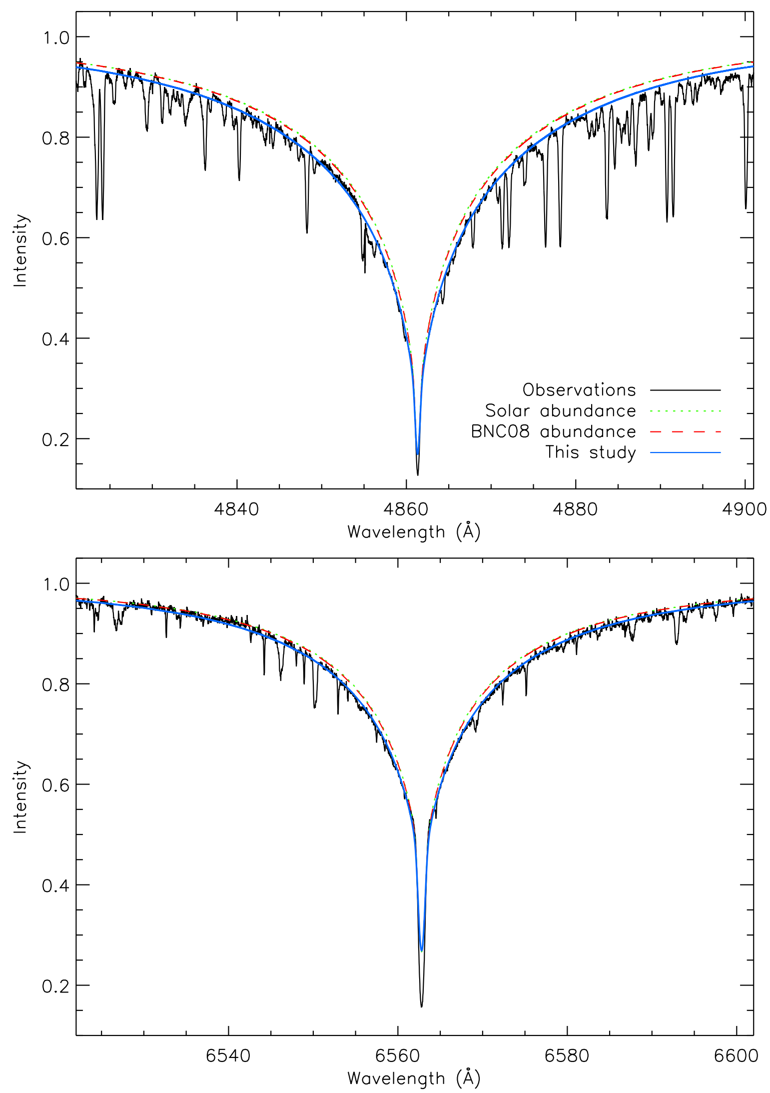

Figure 2: Comparison of the observed and theoretical Hα and Hβ line profiles in α Cir. Observations are marked by the black line. Theoretical calculations with parameters $T_{\rm eff} = 7500$ K, $\log g = 4.1$ are presented for our final self–consistent model atmosphere with the stratification included (the *blue line*), a chemically–homogeneous solar abundance model (the *green line*), and a model computed for the abundances by Bruntt et al. (2008) (the *red line*).

$R = 1.77 \pm 0.04 R_{\odot}$ for HD 24712. The model with the parameters $T_{\rm eff} = 7250$ K, $\log g = 4.1$ reproduces simultaneously the observed photometry, energy distribution, hydrogen line profiles and metallic line spectra, including the REE lines in all ionization stages. Effective temperature of the star did not change compared to the previous analysis (Ryabchikova et al., 1997), while the surface gravity decreased from $\log g = 4.3$ to $\log g = 4.1$.

Saio et al. (2010) performed pulsation modelling of HD 24712 and for the first time modelled not only the observed frequency pattern but also the distribution of the amplitude and phase of the pulsation wave through the stellar atmosphere. These authors used different atmospheric models including a model with the temperature inversion in the upper atmosphere presented above. They found that this model provides a better description of the observed pulsation properties of HD 24712 compared to the model without temperature inversion.

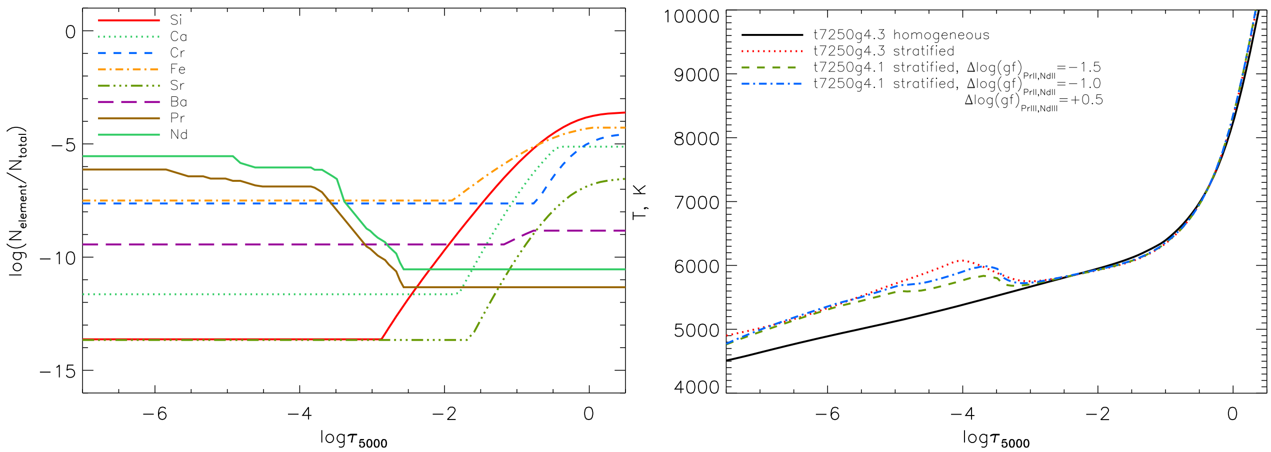

Figure 3: Stratification of eight elements in the atmosphere of HD 24712 derived using the final model with a scaled REE opacity (*left panel*). *Right panel* shows the effect of the Pr and Nd stratification on the model temperature structure. The solid line — t7250g4.3 model calculated with homogeneous abundances; the dotted line — t7250g4.3 model calculated with stratified abundances; the dashed and dash–dotted lines — t7250g4.1 models calculated with stratified abundances and scaled Pr II,III and Nd II,III log(gf)–values.

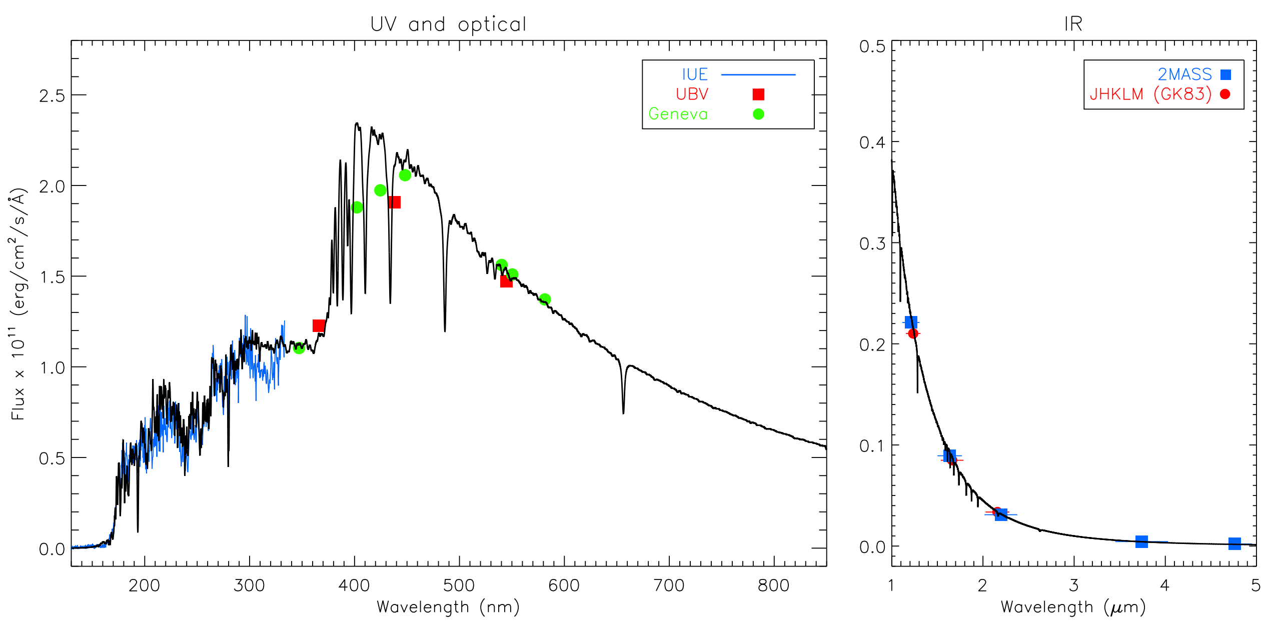

Figure 4: Calculated and observed energy distributions of HD 24712. Solid line — t7250g4.1 model calculated with stratified abundances shown in Fig. 3.

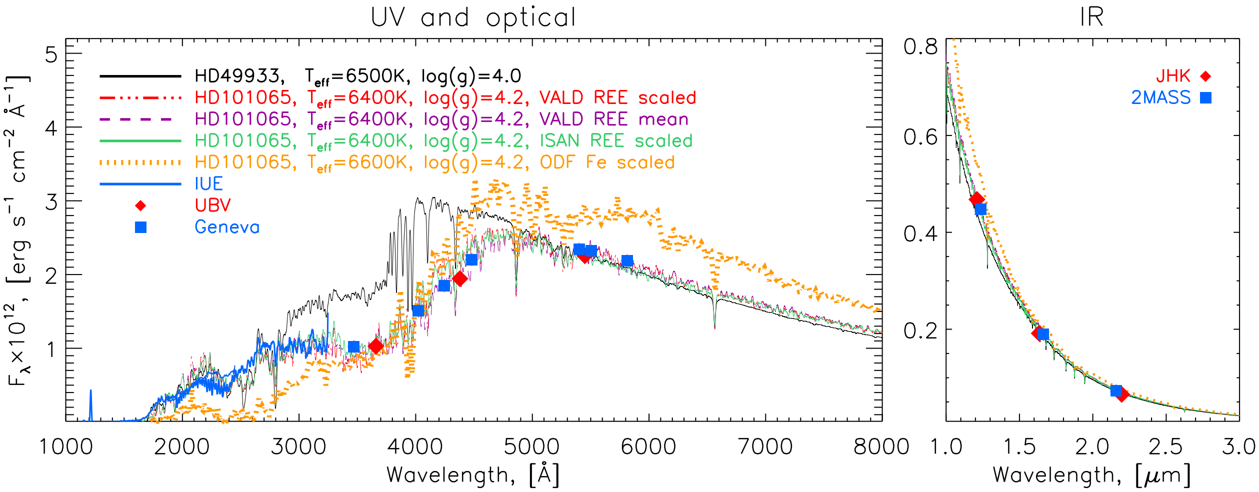

Figure 5: Observed and theoretical energy distributions of HD 101065 calculated with the scaled REE opacity. For comparison purposes the theoretical energy distributions of the previous HD 101065 model and of a normal F–type star HD 49933 are also shown. All the theoretical calculations are smoothed with 20 Å Gaussian.

2.3 HD 101065 (Przybylski' Star)

HD 101065 — the famous Przybylski' star is the one of the most intriguing stars. Formerly, it belonged to the roAp group, but its extremely anomalous spectrum consisting mostly of the REE lines makes this star an unusual object. Previous attempts to model this star (Cowley et al., 2000) failed to reproduce the observed Strömgren colours, in particular, the c_1–index. The best parameters for HD 101065 atmosphere were defined as $T_{\rm eff} = 6600$ K, $\log g = 4.2$. These parameters were recently supported by an independent pulsation modelling. Mkrtichian et al. (2008) made an analysis of the radial velocity (RV) pulsations of this star and modelling of the frequency pattern. They found that the model with the parameters $T_{\rm eff} = 6622 \pm 100$ K, $\log g = 4.06 \pm 0.04$ and $R = 1.90 \pm 0.08 R_\odot$ explains the rich p–mode spectrum observed in HD 101065. However, a problem with the fit to the photometric indices persisted. A new atmospheric modelling of HD 101065 was performed by Shulyak et al. (2010) using millions of predicted REE lines specially calculated for this purpose at the Institute of Spectroscopy of the RAS. It was found that hundreds of thousands of spectral lines of the REE elements Pr, Nd, Sm and Dy contribute to the line opacity in model atmosphere calculations for HD 101065. Shulyak et al. (2010) derived $T_{\rm eff} = 6400$ K and $\log g = 4.2$. While the revised temperature does not change significantly from the previous determination, for the first time Shulyak et al. (2010) managed to represent the observed energy distribution of HD 101065. It is illustrated in Fig. 5 taken from the paper by Shulyak et al. (2010). The stratifications of Si, Ca, Fe, Ba were calculated and taken into account the modelling, however its effect is insignificant compared to the effect of the REE line opacity.

Again, combining our model flux with the Hipparcos parallax $\pi = 8.93 \pm 0.87$ mas (van Leeuwen, 2007) and fitting it to the observed energy distribution one gets a radius estimate $R = 1.98 \pm 0.03 R_\odot$ for HD 101065, a value in excellent agreement with the independent estimate of radius from the pulsation analysis.

2.4 γ Equ

γ Equ is one of the best–studied roAp stars. The first stratification analysis was made by Ryabchikova et al. (2002). The LTE abundance stratification was studied by the trial–and–error method. However, in this paper an existence of the enriched REE layers in the upper atmosphere

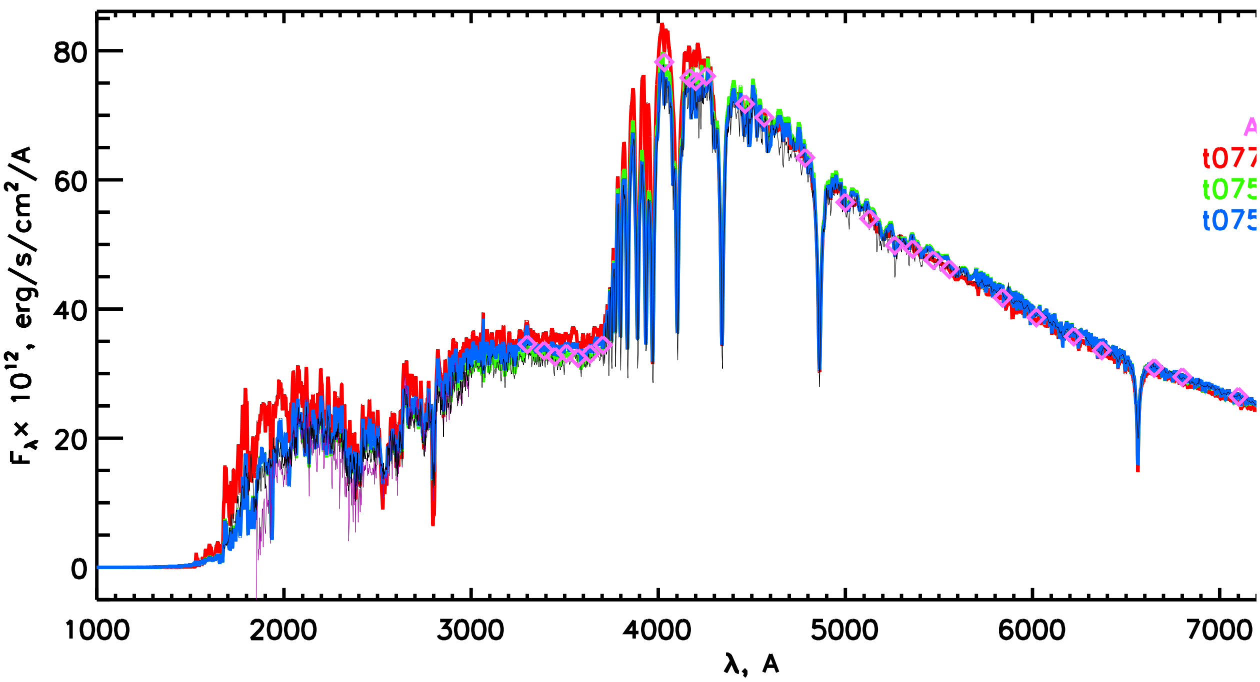

Figure 6: Observed and theoretical energy distributions of γ Equ calculated with the stratification of 17 elements. All theoretical calculations are smoothed with a 20 Å Gaussian.

was proposed for the first time as an explanation of the observed RV pulsational amplitudes and phases. The LLmodels modelling of γ Equ is in progress. We derived the stratification for 17 chemical elements including Mg, Si, Ca, Sc–Ni, Sr–Y–Zr, Ba, Pr and Nd. For Pr and Nd the stratification was derived in the NLTE (Mashonkina et al., 2005, 2009). We started with the atmospheric parameters $T_{\rm eff} = 7700$ K, $\log g = 4.2$ and abundances from Ryabchikova et al. (1997), and calculated a small grid of the models in the $7400-7700$ K temperature range and $\log g = 3.8-4.2$ range. At each iteration we compared a theoretical energy distribution with the observed flux distributions obtained by the STIS in the $1500-10000$ Å region and extracted from the MAST–IUE archive (http://archive.stsci.edu/iue/). We also used spectrophotometry by Adelman (1981). After 3 iterations the models were converged and we obtained the final parameters: $T_{\rm eff} = 7550$ K, and $\log g$ between 3.8 and 4.0. The difference in fitting is negligible. Fig. 6 shows a comparison between the observed flux distribution and the theoretical calculations. Using Hipparcos parallax $\pi = 27.55 \pm 0.62$ mas (van Leeuwen, 2007) we derived the radius of γ Equ as $R = 2.07 \pm 0.05 R_\odot$ from fitting the theoretical flux for the 7550g40 model to the observed flux. The spectroscopically derived value of the radius agrees with the recent interferometric results. Perraut et al. (2010) obtained $R = 2.20 \pm 0.12 R_\odot$.

A detailed analysis and modelling of the atmospheres of Ap stars based on high quality spectroscopic, photometric and spectrophotometry data in a wide spectral range allow us to get accurate estimates for the global stellar parameters such as effective temperature, radius and luminosity. Our results are supported by other independent measurements of the stellar radii: interferometry and/or pulsation analysis.

3 Self–Consistent Diffusion Models

Self–consistent diffusion models are based on the Phoenix (Hauschildt et al., 1999) model atmospheres where the diffusion of 39 chemical elements from He to La is calculated simultaneously and

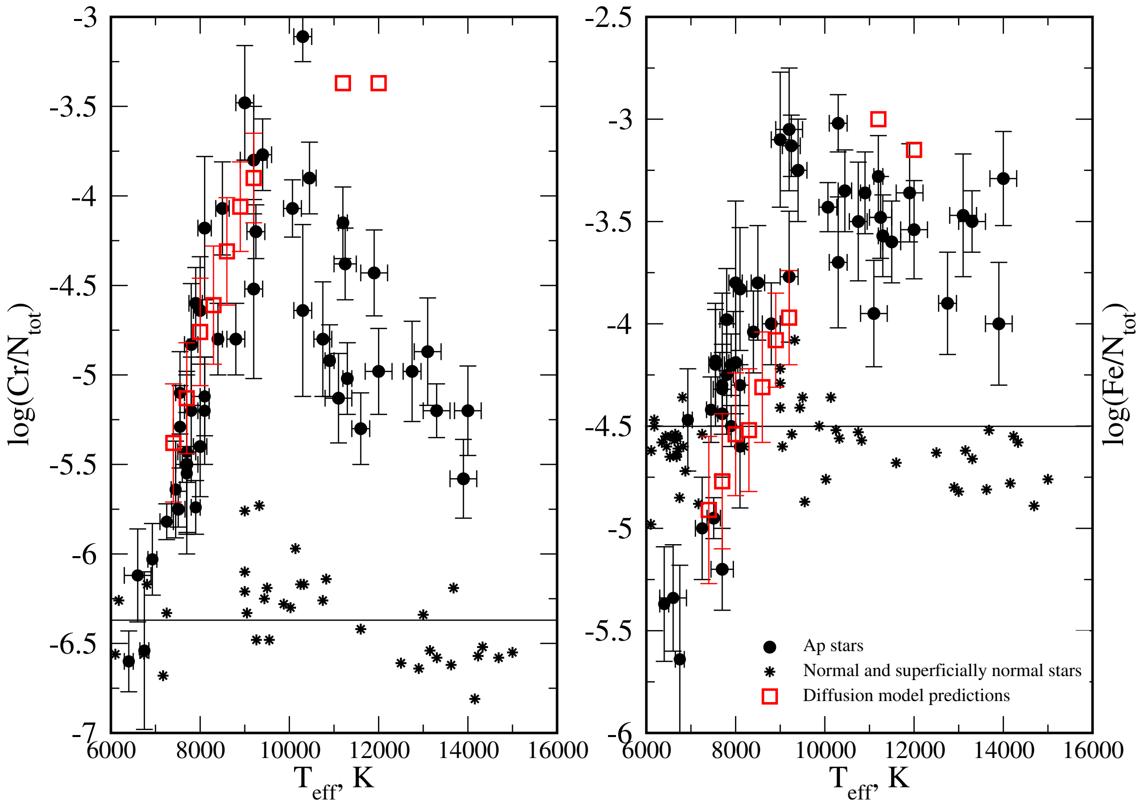

Figure 7: Temperature dependence of the averaged Cr (left panel) and Fe (right panel) abundances in the atmospheres of Ap stars. The red open squares show the same abundances expected in the chemically stratified atmospheres.

self–consistently with the structure of the model atmosphere (Hui–Bon–Hoa et al., 2000; LeBlanc, 2003; LeBlanc & Monin, 2005; LeBlanc et al., 2009). Diffusion calculations start from a model atmosphere with a homogeneous composition assuming the solar abundances. The abundances of the elements are modified to obtain a null diffusion velocity (i. e. equilibrium abundances). The algorithm employed uses an iterative process, where the atmospheric structure is adjusted as the abundances are modified due to diffusion. Therefore, abundance corrections are followed by temperature corrections. In turn, the changes in the physical structure lead to an imbalance of the forces acting on the chemical elements. The diffusion velocities become non–zero, and the abundances must then be corrected again in order to compensate for this imbalance. In order to avoid non–physical situations, the maxima and minima for the abundances are imposed (typically on the order of ± 3 dex from the initial solar abundances). Self–consistent diffusion models were successful in explaining several observational anomalies of blue horizontal–branch stars (Hui–Bon–Hoa et al., 2000; LeBLanc et al., 2010).

A grid of self–consistent diffusion models was calculated for the temperature range of Ap stars (7400 – 12000 K), $\log g = 4.0$. We use this grid to check the possible manifestation of element stratification in a large sample of Ap stars. Ryabchikova (2005) studied temperature dependence of Si, Ca, Cr, Fe averaged abundances in the atmospheres of 46 Ap stars. The temperature behaviour of the Cr and Fe abundances are shown in Fig. 7. Using a grid of self–consistent diffusion models, we synthesised the line profiles of a few representative species Cr I/II, Fe I/II, usually chosen for the abundance determinations. Considering these synthetic line profiles as the observations, we calculated average abundances for each grid temperature in a usual manner using the models with homogeneous abundances. The results of these simulations are plotted by red open squares in Fig. 7.

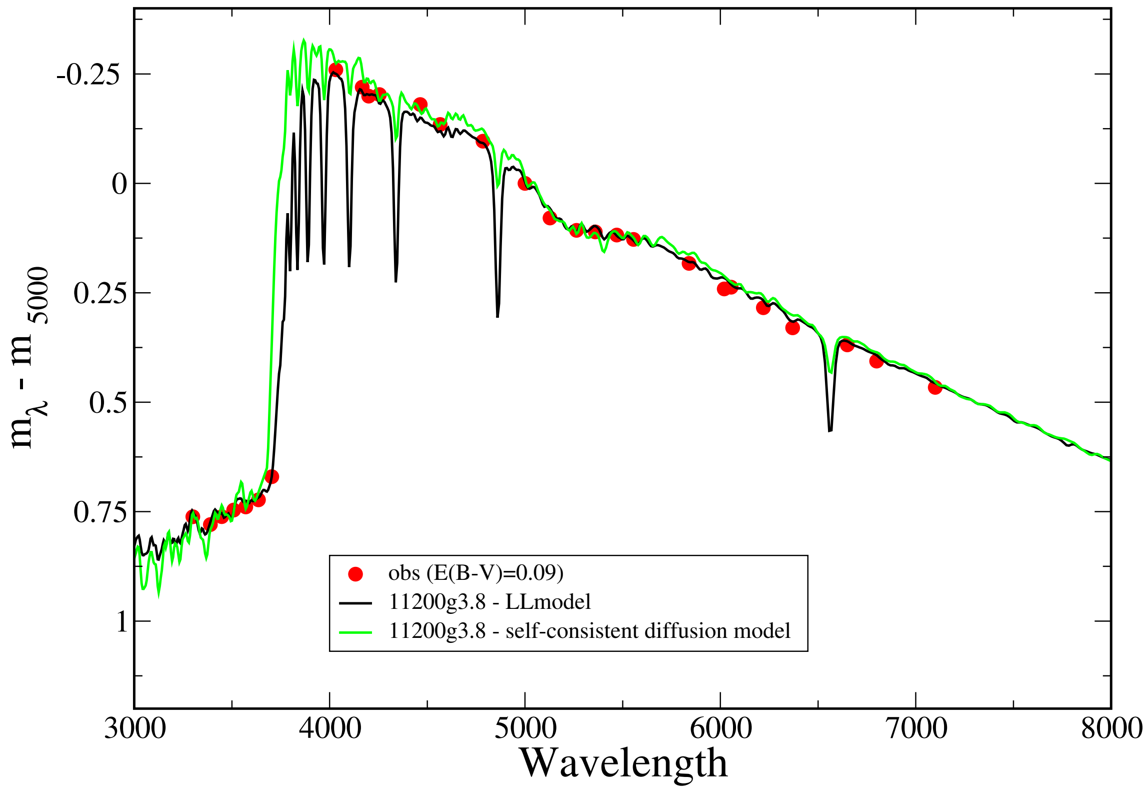

Figure 8: Comparison between the observed and theoretical energy distributions calculated for the homogeneous LLmodels (black line) and the self–consistent diffusion model (green line)

This comparison clearly shows that the observed trend of the averaged abundances with temperature is caused by the diffusion process in the atmospheres of Ap stars.

For one of Ap stars, HD 170973 we constructed and compared a model calculated with the LLmodels code and the self–consistent diffusion model. The abundance analysis of this relatively hot star ($T_{\rm eff} = 10750$ K) was made by López–García et al. (2001) who found it to be overabundant both in the Fe–peak elements and in the REEs. According to self–consistent diffusion calculations, the abundance jumps created by diffusion are much smaller or absent at these temperatures, at least at the atmospheric layers, where most of the optical spectral lines are formed, while the mean overabundance of Fe reaches +1.5 dex, and that of Cr can attain +2 dex. An empirical analysis of the Ca stratification confirmed the absence of Ca gradients (Ryabchikova et al., 2008). The relative sharpness of spectral lines ($v_e \sin i$ = 8.5 km/s) and richness of Fe–peak elements spectra makes HD 170973 an ideal object for the diffusion study in the atmospheres of rapid Ap stars. The UVES spectrum of HD 170973 in 3050 − 9000 Å, used earlier in the Ca stratification analysis (Ryabchikova et al., 2008) was the main source for the present spectroscopic study.

First, a grid of atmospheric models around $T_{\rm eff} = 11000$ K and $\log g$ between 3.5 and 4.0 was calculated with the LLmodels code taking into account individual abundances from López–García et al. (2001) and from Kato (2003). A comparison of the theoretical flux distribution with the one observed spectrophotometry (Adelman, 1983), corrected for interstellar absorption with E(B−V) = 0.09 shows that a model with $T_{\rm eff} = 11200$ K and $\log g = 3.8$ provides a reasonably good fit to the observed energy distribution (the black line on Fig. 8) and hydrogen line profiles. With these parameters we recalculated the abundances in the atmosphere of HD 170973.

Then we calculated the self–consistent diffusion model for the derived atmospheric parameters, where 39 elements (H–Ga, Kr–Nb, Ba and La) were included. As mentioned above, the abundances

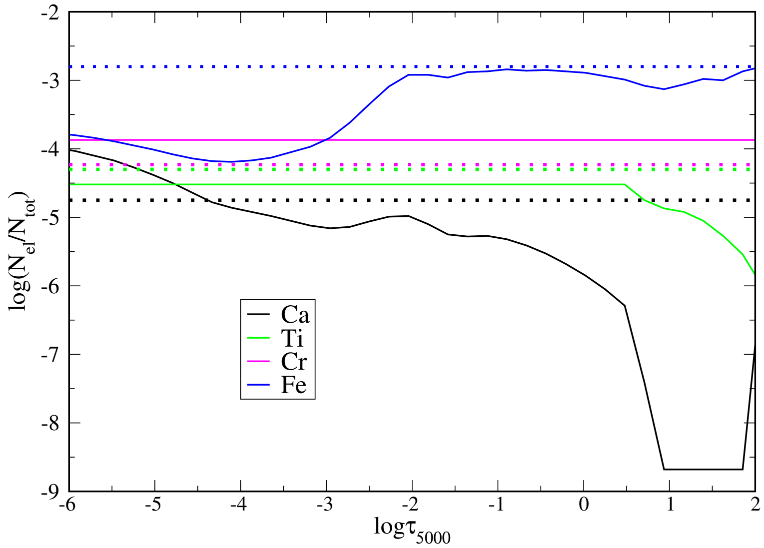

Figure 9: Theoretical abundance distributions of the elements Ca, Ti, Cr and Fe (solid lines). Dotted lines show mean abundances of the same elements derived in HD 170973 with the LLMODELS.

of the elements are modified with the aim of obtaining a null diffusion velocity (i. e. equilibrium abundances). The radiative accelerations for both bound–bound and bound–free transitions are included. These accelerations are calculated on a sufficiently fine frequency grid to assure proper accuracy. In order to avoid non-physical situations, the maxima and minima ± 2.5 dex for the abundances are imposed. (see LeBlanc et al., 2009, for more details). Theoretical flux calculated with the self–consistent diffusion model is shown by the green line in Fig. 8.

Relatively narrow lines in the HD 170973 spectrum allow us to perform a standard abundance analysis based on the equivalent width measurements and the LLMODELS. In total about 1200 spectral lines were measured in the 3050 – 8400 Å region with the main contribution from Ti II, Cr II, Fe II and the lines of the rare–earth elements (REE) in the first and second ionization stages. Detailed results of the spectroscopic study will be presented in a separate paper, here we focus on Cr and Fe. The abundance results for Fe where we managed to derive consistent abundances independently from the lines of three ionization stages provide an additional support to the model atmosphere parameters. Microturbulent velocity is small and does not exceed 0.5 – 0.7 km/s. The empirical stratification analysis made for Cr and Fe does not reveal any significant abundance jumps in the atmosphere of HD 170973.

Theoretical abundance distributions from the self–consistent diffusion model for a few elements are shown in Fig. 9, where the mean abundances for the corresponding elements derived from observations are shown by dotted lines. An excellent agreement is obtained for Fe. In the line forming region, a theoretically predicted overabundance is equal to that derived from spectra. A comparison between the observed profiles (filled circles) and those calculated with a self–consistent diffusion model (red line) are shown in Fig. 10 for a few Fe I and Fe II lines of different intensity lying in extremely different spectral regions and originated from the levels in a wide range of excitation energies.

Diffusion predicts He, C, N, S, Ca, Ti, and Fe abundances comparable with the observed abundances in the atmosphere of HD 170973, however, for many other elements the diffusion predictions are far off. In particular, for all odd Fe–peak elements the diffusion predicts a too high abundance (see Sc II and Mn II lines in Fig. 10). Actually, through the whole atmosphere the radiative forces are capable to support the maximum allowed overabundance of $+2.5$ dex. For the light elements O, Ne, Mg and Si, the diffusion calculations provide a strong depletion in the atmosphere, while the

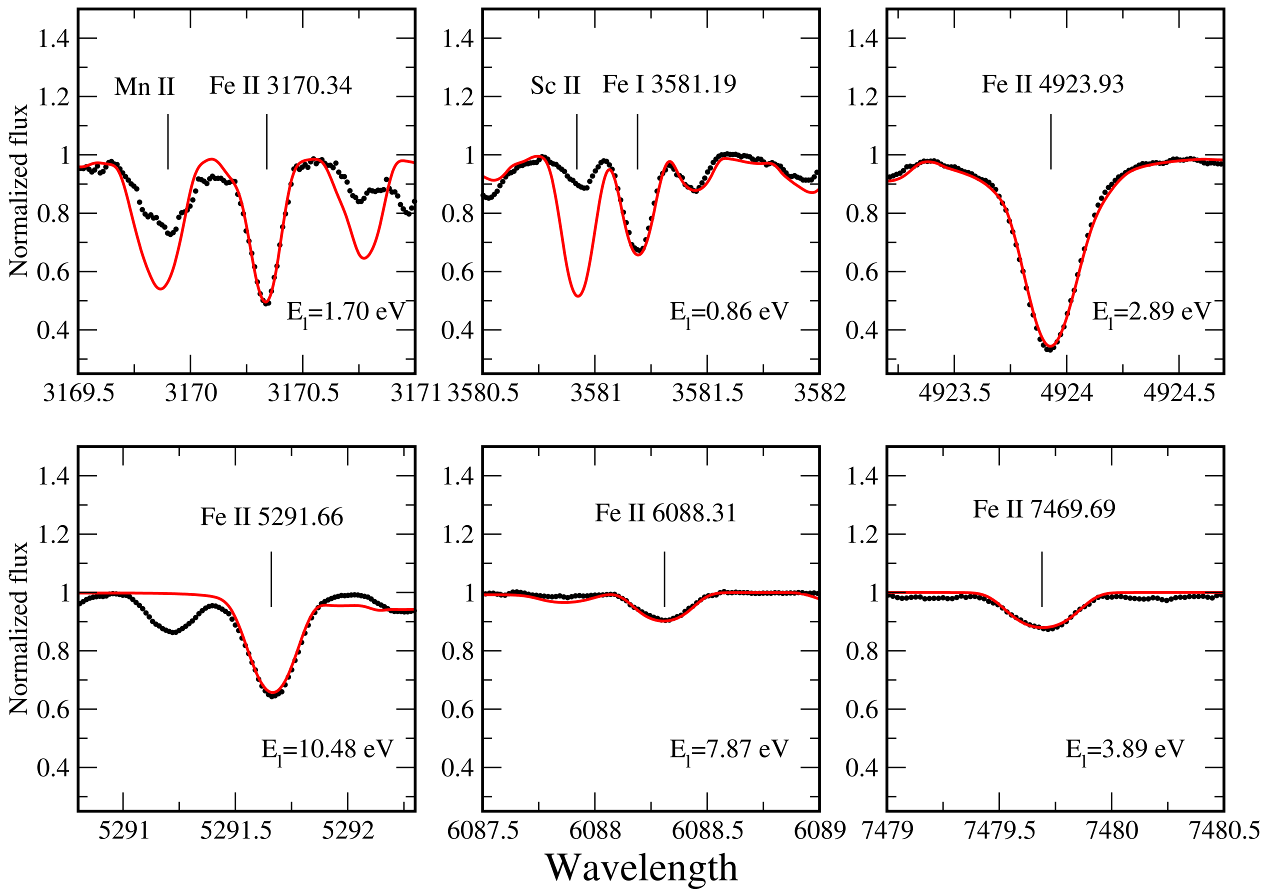

Figure 10: Comparison between the observed (dots) and calculated (solid red line) line profiles of few Fe I and Fe II lines. Calculations are made with the self–consistent diffusion model.

observations show nearly solar abundances or even an overabundance (Si). Such differences between the observations and the theoretical predictions are probably due to the fact that the diffusion models used here are not time–dependent. For instance, in real stars the diffusion occurring below the atmosphere can affect the amount of matter found in the line forming region. However, model atmospheres using the equilibrium abundances are an important first step for the better gauging and for understanding the effect of diffusion in the atmospheres of stars.

4 Conclusions

The development of the new codes for model atmosphere calculations that explicitly take into account all atmospheric abundance anomalies (individual abundances, inhomogeneous element distribution over the atmosphere, magnetic splitting, etc.), affecting the line opacity is a very important step towards a better understanding of the structure of Ap stars. Improved models, calculated with the LLMODELS code are successful in explaining peculiar energy distributions in Ap stars, and provide accurate radius determinations in agreement with the direct interferometric measurements.

The empirically derived element stratifications in the atmospheres of Ap stars are consistent with the self–consistent diffusion calculations of the PHOENIX code. The observed trends of the averaged abundances with temperature follow those, predicted by the diffusion models, providing an additional support for the diffusion process as the main mechanism responsible for the abundance anomalies in the Ap stars.

Acknowledgements. This work was financially supported by the RFBR grants 08–02–00469, 09–02–00002, by the Russian Federal Agency on Science and Innovation grant No. 02.740.11.0247, by the Natural Science and Engineering Research Council of Canada (NSERC) and by Deutsche Forschungsgemeinschaft (DFG) Research Grant RE1664/7–1. We are also thankful to the Réseau québécois de calcul de haute performance (RQCHP) and the Institute of Astronomy of the University of Vienna for computational resources.

References

Adelman S. J. 1981, A&AS, 44, 265

Adelman S. J. 1983, A&AS, 51, 511

Alecian G., Stift M. J., 2007, A&A, 475, 659

Alecian G., Stift M. J., 2010, A&A, 516, A53

Alekseeva G. A., Arkharov A. A., Galkin V. D., Hagen–Thorn E. I., Nikanorova I. N., Novikov V. V., Novopashenny V. B., Pakhomov V. P., Ruban E. V., Shchegolev D. E., 1996, Baltic Astronomy, 5, 603

Babel J., 1992, A&A, 258, 645

Bruntt H., North J. R., Cunha M., Brandão I. M., Elkin V. G., Kurtz D. W., Davis J., Bedding T. R., Jacob A. P., Owens S. M., Robertson J. G., Tango W. J., Gameiro J. F., Ireland M. J., Tuthill P. G., 2008, MNRAS, 386, 2039

Burnashev V. I., 1985, Abastumanskaya Astrofiz. Obs. Byull., 59, 83

Cowley C. R., Ryabchikova T., Kupka F., Bord D. J., Mathys G., Bidelman W. P., 2000, MNRAS, 317, 299

Hauschildt P. H., Allard F., Baron E., 2000, ApJ, 512, 377

Hui–Bon–Hoa A., LeBlanc F., Hauschildt P. H., 2000, ApJ, 535, L43

Kato K., 2003, PASJ, 55, 1133

Kochukhov O., Shulyak D., Ryabchikova T., 2009, A&A, 499, 851

Kupka F., Ryabchikova T. A., Weiss W. W., Kuschnig R., Rogl J., Mathys G., 1996, A&A, 308, 886

LeBlanc F., 2003, ASP Conf. Ser., 305, 206

LeBlanc F., Hui–Bon–Hoa A., Khalack V. R., 2010, MNRAS, 409 1606

LeBlanc F., Monin D., 2003, J. R. Astron. Soc. Can., 99, 139

LeBlanc F., Monin D., Hui–Bon–Hoa A., Hauschildt P. H., 2009, A&A, 495, 937

López–García Z., Adelman S. J., Pintado O. I. 2001, A&A, 367, 859

Mashonkina L., Ryabchikova T., Ryabtsev A., 2005, A&A, 441, 309

Mashonkina L., Ryabchikova T., Ryabtsev A., Kildiyarova R., 2009, A&A, 495, 297

Michaud G., 1970, ApJ, 160, 641

Mkrtichian D. T., Hatzes A. P., Saio H., Shobbrock R. R., 2008, A&A, 490, 1109

Perraut K., Brandão I., Mourard D., Cunha M., Bério Ph., Bonneau D., Chesneau O., Clausse J. M., Delaa O., Marcotto A., Roussel A., Spang A., Stee Ph., Tallon–Bosc I., McAlister H., Ten Brummelaar T., Sturmann J., Sturmann L., Turner N., Farrington C., Goldfinger P. J., 2010, A&A, 526, A89

Ryabchikova T. A., Adelman S. J., Weiss W. W., Kuschnig R., 1997, A&A, 322, 234

Ryabchikova T., Kochukhov O., Bagnulo S., 2008, A&A, 480, 811

Ryabchikova T. A., Landstreet J. D., Gelbmann M. J., Bolgova G. T., Tsymbal V. V., Weiss W. W., 1997, A&A, 327, 1137

Ryabchikova T., Leone F., Kochukhov O., 2005, A&A, 438, 973

Ryabchikova T., Piskunov N., Kochukhov O., Tsymbal V., Mittermayer P., Weiss W. W., 2002, A&A, 384, 545

Saio H., Ryabchikova T., Sachkov M., 2010, MNRAS, 403, 1729

Shulyak D., Ryabchikova T., Kildiyarova R., Kochukhov O., 2010, A&A, 520, A88

Shulyak D., Ryabchikova T., Mashonkina L., Kochukhov O., 2009, A&A, 499, 879

Shulyak D., Tsymbal V., Ryabchikova T., Stütz C., Weiss W. W., 2004, A&A, 428, 993

van Leeuwen F., 2007, Hipparcos, the New Reduction of Raw Data, Astrophysics and Space Science Library, Springer, 350

Wade G. A., Ryabchikova T. A., Bagnulo S., Piskunov N., 2001, ASP Conf. Ser., 248, 373